Journal of Medical Imaging

MedicalImaging.SPIEDigitalLibrary.org

Quantitative analysis of rib kinematics based on dynamic chest bone images: preliminary results

Rie Tanaka
Shigeru Sanada
Keita Sakuta
Hiroki Kawashima

SPIE.

Journal of Medical Imaging 2(2), 024002 (Apr–Jun 2015)

Quantitative analysis of rib kinematics based on dynamic chest bone images: preliminary results

Rie Tanaka,[a,*] Shigeru Sanada,[a] Keita Sakuta,[b] and Hiroki Kawashima[b]
[a]Kanazawa University, College of Medical, Pharmaceutical, and Health Sciences, School of Health Sciences, 5-11-80 Kodatsuno, Kanazawa 920-0942, Japan
[b]Kanazawa University Hospital, Department of Radiology, 13-1 Takara-machi, Kanazawa 920-8641, Japan

Abstract. An image-processing technique for separating bones from soft tissue in static chest radiographs has been developed. The present study was performed to evaluate the usefulness of dynamic bone images in quantitative analysis of rib movement. Dynamic chest radiographs of 16 patients were obtained using a dynamic flat-panel detector and processed to create bone images by using commercial software (Clear Read BS, Riverain Technologies). Velocity vectors were measured in local areas on the dynamic images, which formed a map. The velocity maps obtained with bone and original images for scoliosis and normal cases were compared to assess the advantages of bone images. With dynamic bone images, we were able to quantify and distinguish movements of ribs from those of other lung structures accurately. Limited rib movements of scoliosis patients appeared as a reduced rib velocity field, resulting in an asymmetrical distribution of rib movement. Vector maps in all normal cases exhibited left/right symmetric distributions of the velocity field, whereas those in abnormal cases showed asymmetric distributions because of locally limited rib movements. Dynamic bone images were useful for accurate quantitative analysis of rib movements. The present method has a potential for an additional functional examination in chest radiography. [DOI: 10.1117/1.JMI.2.2.024002]

Keywords: dynamic chest radiography; bone suppression; bone images; rib movement; vector analysis; flat-panel detector.

Paper 15024R received Feb. 10, 2015; accepted for publication Apr. 13, 2015; published online May 7, 2015.

1 Introduction

The thorax, which consists of the rib cage and the respiratory muscles, serves as the respiratory pump that generates movement of air into the lungs while preventing their total collapse during exhalation.[1] Vertebral deformity and traumatic bone fracture limit rib mobility during respiration, resulting in a decrease in vital capacity (VC). In fact, several studies indicated that lung volume and rib mobility are significantly impaired in patients with thoracic kyphosis because of changes in the position of the rib neck,[2,3] and limited rib mobility directly leads to a reduction in pulmonary function in scoliosis cases.[4] Thus, analysis of rib kinematics can contribute to an evaluation of pulmonary function. On the other hand, pulmonary impairments alter lung behavior, resulting in a phase shift and/or extension of the respiratory period. Hence, abnormal motion of the chest wall is very common in patients with chronic obstructive pulmonary diseases.[5,6] As shown in these previous studies, an understanding of rib kinematics is crucial to evaluate the pulmonary function and treatment effects in such cases.[7]

Several approaches have been suggested for the evaluation of rib and chest wall movement, such as plethysmography,[8,9] magnetic resonance imaging (MRI),[10] computed tomography (CT),[11,12] and fluoroscopy. However, plethysmography is an indirect measurement technique, which has limited precision because of changes in results depending on marker placement. MRI provides quasikinematic information only on a specified section, CT involves higher patient exposure dose, and fluoroscopy provides subjective observation. To resolve these problems, a method involving dynamic chest radiography with a flat-panel detector (FPD) combined with computer analysis has been developed over the last decade.[13–15] This method was expected to be useful as an additional examination in chest radiography. However, it has not yet been commonly adopted in clinical settings because of the technical limitations related to the shadows of lung vessels and bronchi overlapping ribs thus preventing accurate quantitative analysis of rib movement.

Recently, an image-processing technique for separating bones from soft tissue in static chest radiographs, called the "bone suppression technique," has been developed.[16] This technique creates both a soft-tissue image and bone image from a conventional chest radiograph, which is usually obtained by the dual-energy subtraction technique, without requiring additional exposure and special equipment. This technique has already been commercially developed and shown to improve radiologists' sensitivity for the detection of lung nodules.[17,18] A recent study investigated an application of the bone suppression technique to chest fluoroscopy, and the usefulness of "dynamic soft-tissue images" in real-time tracking radiation therapy was reported.[19] However, there have been no reports of a clinical application of "dynamic bone images." The major factors responsible for errors in vector analysis of rib movement are the motions of other structures, such as the diaphragm, heart wall, lung vessels, and bronchi. Thus, dynamic bone images may be useful to improve the accuracy of a quantitative analysis of rib

*Address all correspondence to: Rie Tanaka, E-mail: rie44@mhs.mp.kanazawa-u.ac.jp

2329-4302/2015/$25.00 © 2015 SPIE

movement in areas where pulmonary vessels, bronchi, diaphragm, heart wall, and ribs move in a complex manner. The present study was performed to evaluate the usefulness of dynamic bone images in a quantitative analysis of rib movement. This is the first report to date of the creation of dynamic bone images using the bone suppression technique followed by analysis of rib kinematics on the bone images. We demonstrate the potential usefulness of dynamic bone images and several issues to be solved for clinical implementation.

2 Materials and Methods

2.1 *Subjects*

Approval for the study was obtained from our institutional review board, and written informed consent was obtained from all patients prior to inclusion. Dynamic chest radiographs of 16 subjects (abnormal, $n = 6$; normal controls, $n = 10$) were obtained in this preliminary study (Table 1). All of the abnormal subjects were follow-up patients with scoliosis and showed a reduced VC on a pulmonary functional test (PFT). The normal controls had no underlying pulmonary diseases or smoking history, and they were confirmed to be normal based on the chest radiographs and the results of PFT.

2.2 *Image Acquisition*

Dynamic chest radiographs were obtained using a dynamic FPD (Test model; Canon Inc., Tokyo, Japan), x-ray device (KXO 80G; Toshiba, Tokyo, Japan), and x-ray tube (DRX 2724HD 0.6/1.2; Toshiba). The FPD system was an indirect type made of GOS (Gd2O2S:Tb), and exposure conditions were as follows: 110 kV, 80 mA, 6.3 ms, 3 frames per second (fps), source to detector distance 2 m, and a 2-mm Al filter. Posterior–anterior dynamic chest radiographs consisting of 30 frames in 10 s were obtained during a whole breathing cycle in a standing position. The entrance surface dose for 30 frames, measured in air without backscattering, was approximately 0.4 mGy, which was less than that in lateral chest radiography determined as the guidance level of the International Atomic Energy Agency (IAEA) (1.5 mGy).[20] The subjects were instructed to respire according to an automated voice to maintain reproducibility and include both respiratory phases in dynamic images. They practiced the breathing method along with the automated voice before imaging. The matrix size was

Table 1 Subject characteristics.

				Pulmonary functional test		Diaphragm excursion (cm)	
	Patient No.	Age	Sex	VC (L)	FEV1.0 (L)	R	L
Abnormal cases	1	75	F	1.1	1.1	0.9	2.0
	2	21	M	3.6	3.1	3.9	3.7
	3	40	F	1.0	1.5	2.3	1.4
	4	62	M	2.4	1.2	1.7	2.5
	5	61	F	2.9	1.9	3.0	3.5
	6	77	M	3.0	0.7	0.8	1.2
Average		$56.0 + 21.7$		$2.4 + 1.1$	$1.6 + 0.9$	$2.1 + 1.2$	$2.4 + 1.1$
Normal controls	7	53	M	4.9	3.5	3.5	3.1
	8	43	M	5.6	4.3	2.8	4.0
	9	22	M	4.7	4.0	6.1	5.6
	10	56	M	5.3	3.7	2.3	2.4
	11	22	M	4.4	4.0	4.0	4.2
	12	20	M	4.3	3.9	3.9	4.0
	13	24	M	5.9	4.9	2.3	3.0
	14	24	M	5.6	4.3	3.6	4.5
	15	30	M	4.8	3.9	3.4	3.4
	16	21	M	4.3	3.9	3.4	3.8
Average		31.5 ± 13.9		5.0 ± 0.6	4.0 ± 0.4	3.5 ± 1.1	3.8 ± 0.9

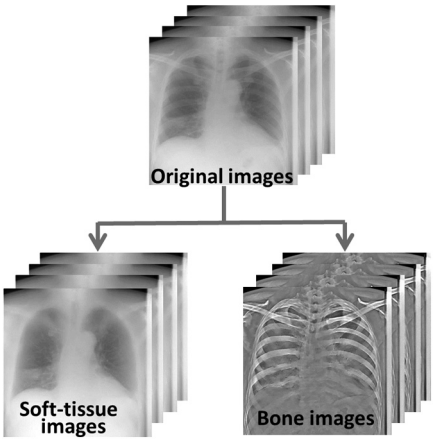

Fig. 1 Dynamic soft tissue and bone images generated from dynamic chest radiographs based on the bone suppression technique.

1344×1344 pixels, the pixel size was 320×320 μm, and the gray level range of the images was 4096.

2.3 *Creation of Bone Images*

Bone images were created by using commercial bone suppression image-processing software (Clear Read Bone Suppression; Riverain Technologies, Miamisburg, Ohio). This technique was originally developed for suppressing the contrast of ribs and clavicles by using image-processing techniques and regression-based artificial neural network (ANN) machine learning methods.[16] In this method, ANN models are trained using normalized input chest radiographs and normalized teaching images obtained from dual-energy subtraction devices. The method uses ANN models along with several image feature representations to accurately estimate the fraction of each input pixel associated with bone and soft tissue. After developing the model-based training set, the models estimate "bone-image-like" images from the input chest images. By subtracting the "bone-image-like" images from the chest radiographs, "soft-tissue-image-like" images are formed, where the ribs and clavicles are substantially suppressed. In this study, we used "bone-image-like" images provided during the creation of "soft-tissue-image-like" images.

For bone suppression image processing, a sequential image file was separated into multiple DICOM files with a unique service object pair instance unique identifier. The commercial bone suppression image-processing software was applied to the dynamic chest radiographs to create corresponding bone images (Fig. 1). In this system, a bone suppression image is created from an original image. Thus, the sequential bone suppression images were produced in the same number as the original ones. The resulting bone suppression images were output in the default contrast mode in the system.

2.4 *Image Analysis*

In many cases, body motion was not observed because the anterior chest wall was in close contact with the surface of FPD. However, in case that body motion was observed, we manually correct it by shifting or rotating images before the vector analysis. For local vector analysis, the dynamic bone images were divided into block units [Fig. 2(a)] with the block size set to be almost the same as the intercostal space such that each rib

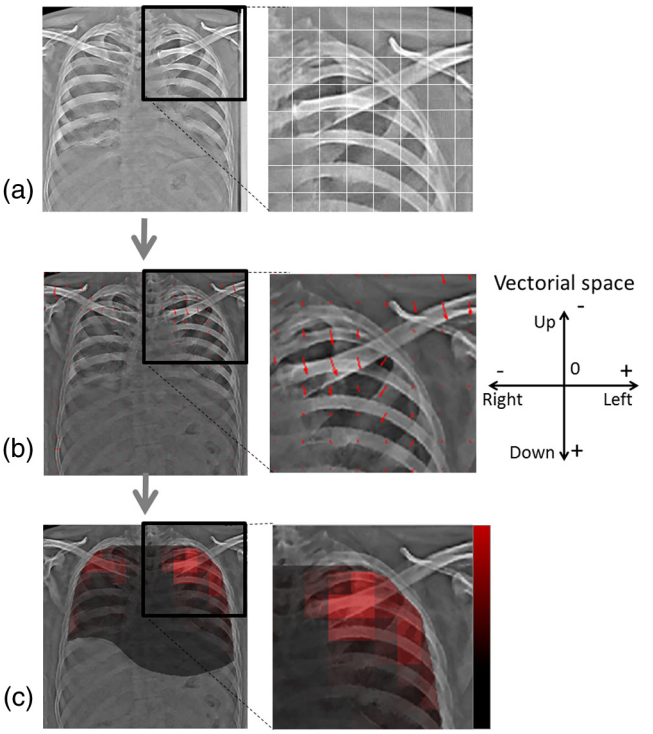

Fig. 2 Process for vector analysis of dynamic bone images. (a) One frame of dynamic bone image. The white solid lines indicate local areas for measurement of the velocity vector in block units. (b) One frame of the velocity vector map and partially enlarged view. Arrows indicate vector velocity in each local area. (c) One frame of the velocity magnitude map and partially enlarged view. Lighter color indicates high speed, whereas darker color indicates low speed.

motion can be analyzed separately in each block.[13,21] Velocity vectors, i.e., vector field, were measured in each block to estimate the direction and speed of rib motion from one image to another (MATLAB ver. 2012b; MathWorks, Natick, Massachusetts).[22,23] Normal rib kinetics indicates the symmetry in both hemithoraces and synchronization with the respiratory phase.[1] Thus, to assess the rib kinetics quantitatively, the velocity vectors were summed up in the horizontal and vertical directions, respectively. If the rib kinetics was normal, the vector sum in the vertical direction should change in synchrony with the respiratory phase, whereas the vector sum in the horizontal direction should be zero irrespective of the respiratory phase because of the symmetrically moving directions in both hemithoraces.

To facilitate visual evaluation, the measured vectors were superimposed on the bone images in the form of small arrows and the resulting images provided the "velocity vector map" [Fig. 2(b)]. The magnitudes of the vectors were also calculated, and then superimposed on dynamic bone images in the form of a color display [Fig. 2(c)]. In the resulting "velocity magnitude map," lighter-colored areas contained high-speed rib motion, whereas darker-colored areas contained low-speed rib motion. The distance from the lung apex to the diaphragm was measured throughout all the frames for using as an index of respiratory phase and for the calculation of diaphragm excursion.[14]

2.5 *Clinical Evaluation*

To investigate the clinical usefulness of the present method, a "velocity vector map" and "velocity magnitude map" were evaluated in terms of the distribution of the velocity field and

consistency with rib kinetics.[4] In addition, the symmetry in both hemithoraces was assessed based on the vector sum in the horizontal and vertical directions, whereas synchronization with respiratory phase was assessed based on the correlation coefficient between the diaphragm displacement (per frame) and vector sum in the vertical direction in each frame.

3 Results

Dynamic bone images with a large field of view could permit direct comparison of right and left rib movements in one imaging procedure. We were able to quantify and distinguish movements of ribs from those of other lung structures accurately based on dynamic bone images.

Figures 3 and 4 show the results of velocity vector analysis in three normal controls (patient Nos. 7, 8, and 9). The direction of rib movement during inspiration was oblique, upward, and outward, while the movement during expiration was oblique, downward, and inward, as shown in the velocity vector maps in Fig. 3. The findings were symmetrical in both hemithoraces throughout respiration. The displacement of rib movement around the external wall was larger than those around the body axis and was also symmetrical in both hemithoraces, as shown in the magnitude maps in Fig. 3. On the other hand, the movements of the other structures, such as the diaphragm and heart wall, were dominantly revealed on both velocity vector maps and vector magnitude maps generated from conventional dynamic chest images. Such left/right symmetry of rib kinetics was not observed in those images (Fig. 4).

Figure 5 shows the vector sum in the horizontal and vertical directions during respiration in the same normal controls as Figs. 3 and 4. The vector sum in the vertical direction was in synchrony with the respiratory phase, with positive and negative values in the expiratory and inspiratory phases, respectively. There was a high correlation between the diaphragm displacement (per frame) and vector sum in the vertical direction in each frame (Fig. 6). In contrast, the vector sum in the horizontal direction was considerably small irrespective of respiratory phase.

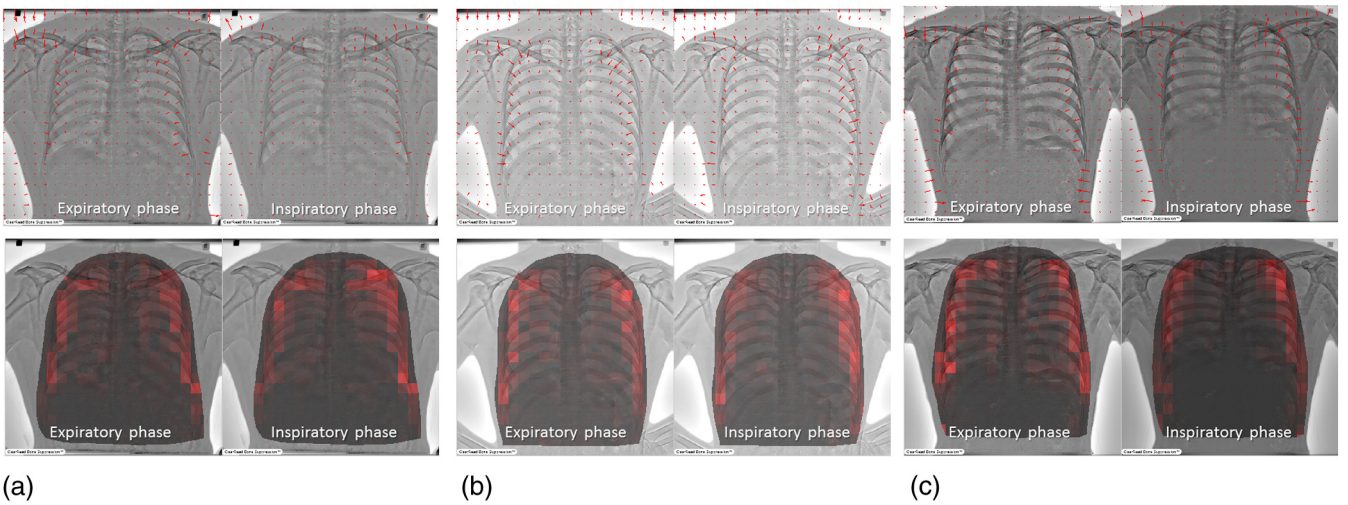

Fig. 3 Velocity vector map (upper) and vector magnitude map (lower) generated based on velocity vector analysis on dynamic bone images (normal controls). (a) A 53-year-old man. (b) A 43-year-old man. (c) A 22-year-old man.

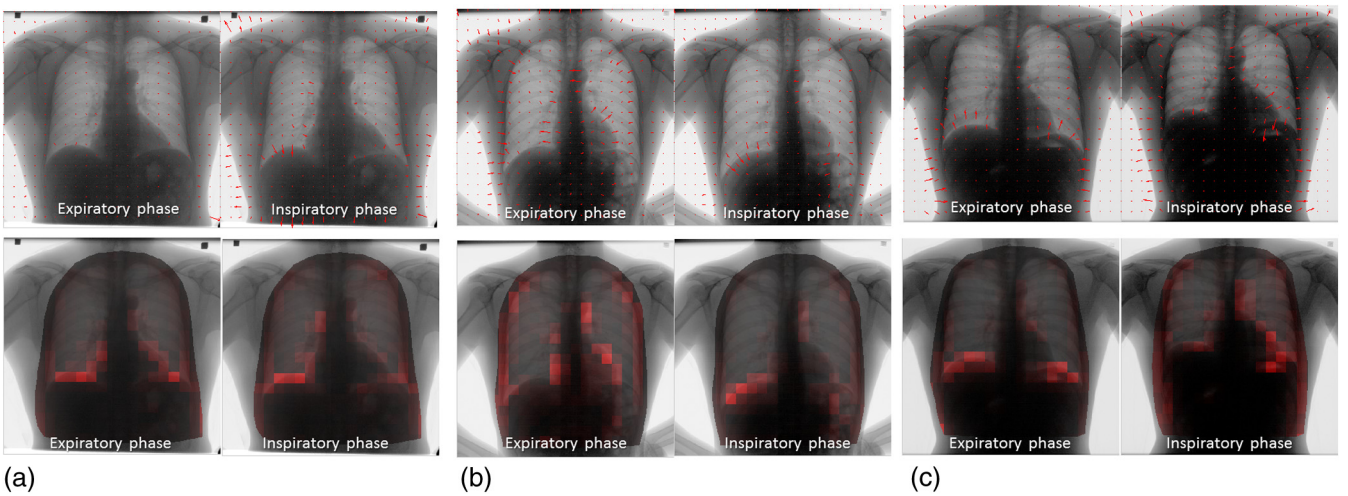

Fig. 4 Velocity vector map (upper) and vector magnitude map (lower) generated based on velocity vector analysis on conventional dynamic chest images (normal controls). (a) A 53-year-old man. (b) A 43-year-old man. (c) A 22-year-old man.

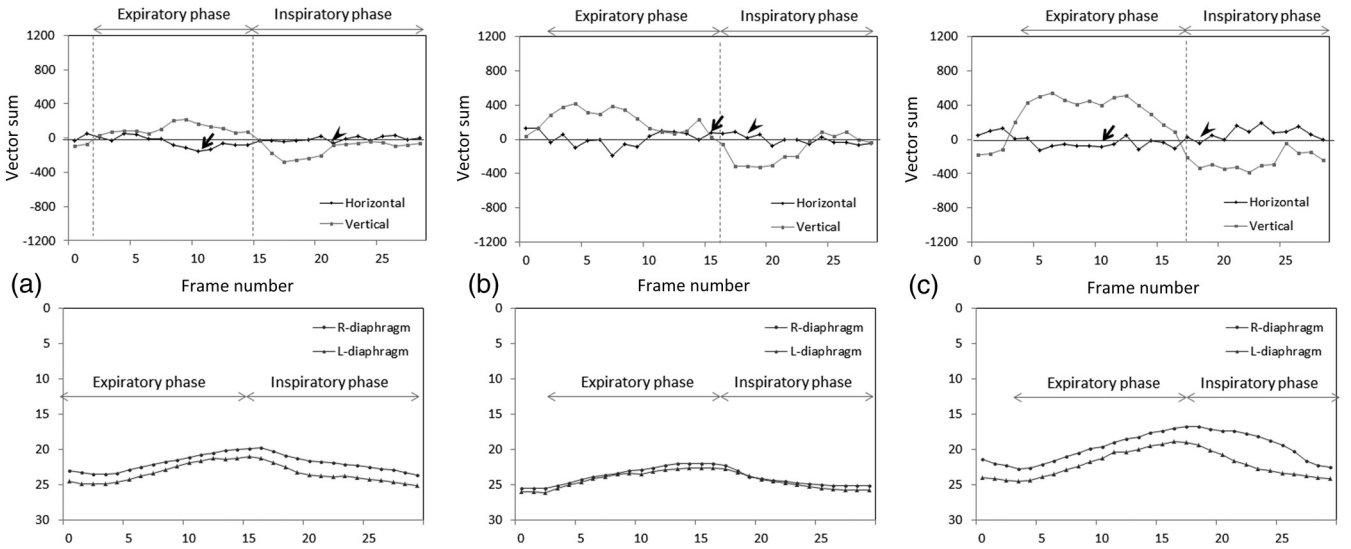

Fig. 5 Vector sum in the horizontal and vertical directions (normal controls). (a) A 53-year-old man. (b) A 43-year-old man. (c) A 22-year-old man. The arrows and arrow heads show the frames in expiratory and inspiratory phases indicated in Figs. 3 and 4, respectively.

Figure 7 shows the variation of vector sum in the horizontal direction throughout all the frames. Normal controls were more likely to show small variations.

Figure 8 shows the resulting maps in three abnormal subjects (patient Nos. 1, 2, and 3). Limited rib mobility appeared as a reduced velocity field, resulting in an asymmetrical distribution of rib movement in both the velocity vector maps and velocity magnitude maps created from the dynamic bone images. Furthermore, paradoxical rib movements were observed in some frames, as shown in Fig. 8(a). In this case, ribs moving downward and inward and ribs moving upward and outward were found in the inspiratory phase. However, these abnormalities could not be observed in those generated from conventional dynamic chest images (Fig. 9) because of the motion of other structures such as the diaphragm, heart wall, lung vessels, and bronchi.

Figure 10 shows the vector sum in each direction in the same abnormal cases as Figs. 8 and 9. The vector sum in the vertical direction showed less synchrony with the respiratory phase, and three out of six abnormal cases showed no correlation with the diaphragm movements (Fig. 6). There was a significant difference between normal and abnormal cases ($P < 0.01$). The vector sum in the horizontal direction sometimes showed a large deviation from the horizontal axis, representing the vector sum of zero. Such a large deviation was always found in the frame with asymmetrical distribution of rib movement, as shown in Fig. 8. Abnormal cases were more likely to show large variations of the vector sum in the horizontal direction throughout all the frames.

4 Discussion

The results of the present preliminary study indicated that velocity vector analysis on dynamic bone images has the potential to allow direct and rapid evaluation of respiratory rib kinetics. The major factors responsible for vector analysis errors of rib movement were the motions of other structures, such as the diaphragm, heart wall, lung vessels, and bronchi. Low image quality in the mediastinum could be another factor to cause vector

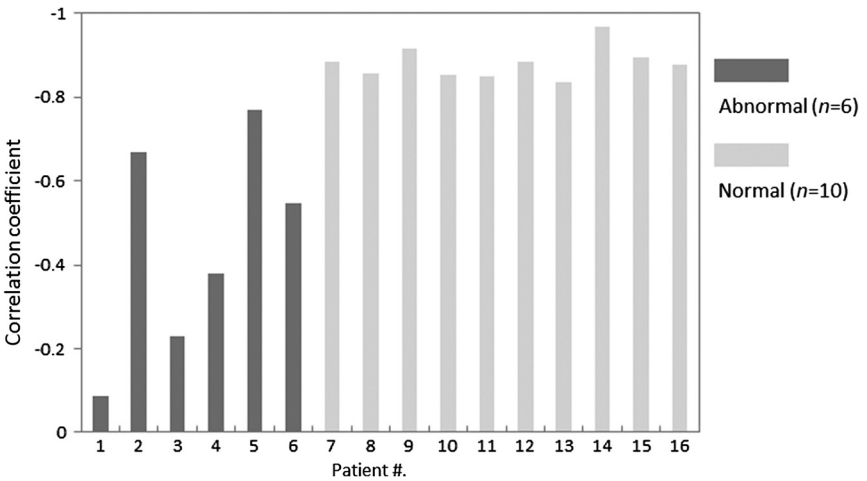

Fig. 6 Correlation coefficient between the diaphragm displacement (per frame) and vector sum in the vertical direction in each frame.

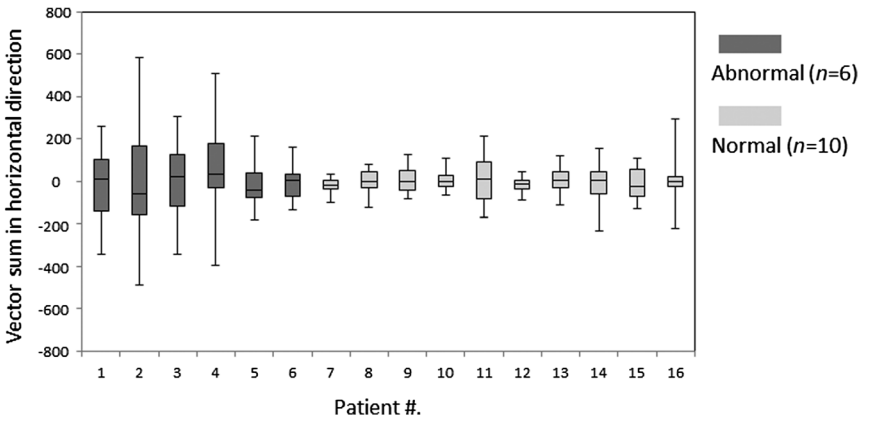

Fig. 7 Variation of vector sum in the horizontal direction.

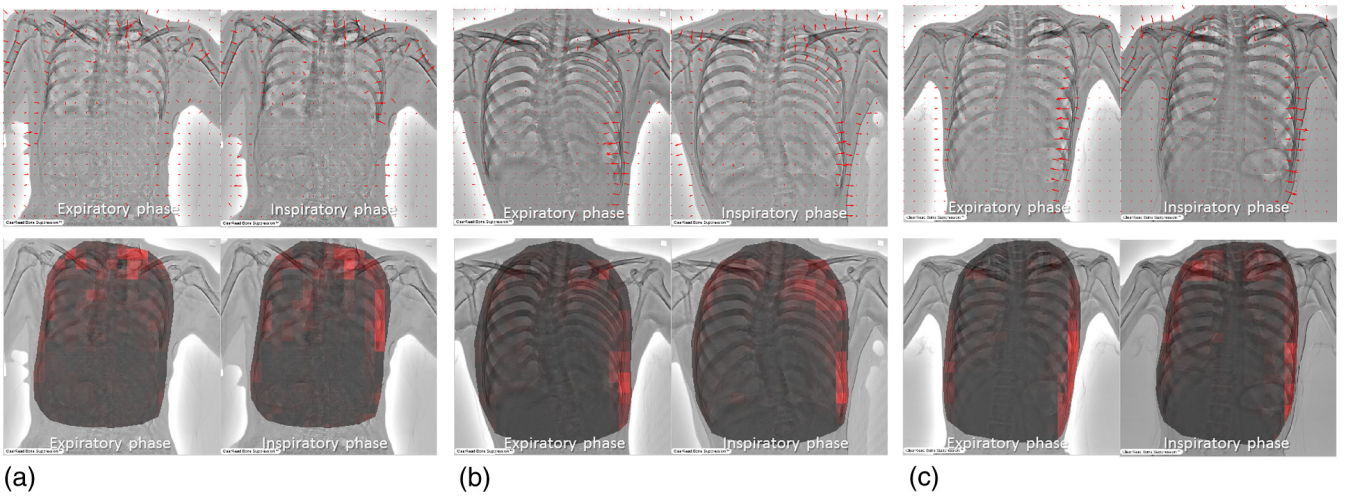

Fig. 8 Velocity vector map (upper) and vector magnitude map (lower) generated based on velocity vector analysis on dynamic bone images (abnormal subjects). (a) A 75-year-old woman. (b) A 21-year-old man. (c) A 40-year-old woman.

analysis errors. Such lung structures were eliminated and rib movement was able to be selectively analyzed based on bone images. Thus, the bone suppression technique was effective in areas with complex and/or dynamic movement of such lung structures. Furthermore, our computerized method provided quantitative data regarding the direction and speed of rib movements and allowed their visualization as vector maps. These maps were very useful to understand rib kinetics and estimate pulmonary function. In the previous method with conventional dynamic images, rib movements could not be quantified separately from those of the other lung structures,[13–15] and provided mixed vector fields, which were not meaningful for understanding rib movements. Dynamic bone images rendered it possible to quantify and visualize rib movements separately from those of the other lung structures, thus yielding meaningful diagnostic information on rib movements.

Vector maps in all normal cases revealed left/right symmetric distributions of the velocity field, whereas those in abnormal cases showed asymmetric distributions because of reduced rib movements. The findings were supported by the rib kinetics reported previously.[4] These results indicated that abnormal rib movement could be differentiated from normal movement based on deviation from uniformity and right/left symmetry of the velocity field on dynamic bone images. In this study, we developed an index that quantitatively measures the contralateral asymmetry of the velocity vector for differentiating abnormal rib kinetics from normal one. The symmetry in both hemithoraces of rib kinetics and its synchronization with respiratory phase were successfully assessed based on the vector sum in the horizontal and vertical directions, respectively. In fact, asymmetrical distribution of rib movement as shown in Fig. 8 always showed a large vector sum in the horizontal direction. These results indicated that the vector sum is a promising and simple index to evaluate rib kinetics.

This is the first report to indicate the clinical usefulness of rib kinematics obtained from soft-tissue-suppressed dynamic chest radiography for identifying abnormality in the lungs. However, this pilot study had several limitations in sample size and ground truth. The number of clinical cases is not sufficient to establish a concrete normal pattern basis and diagnostic criteria. In addition, the present method evaluated the estimated findings that rib mobility is impaired because of changes in the position of the rib neck, which leads to a reduction in pulmonary function.[2–4] Further studies in larger numbers of subjects with concrete ground truth are required along with investigations of the ability of our method to detect abnormalities. There were also

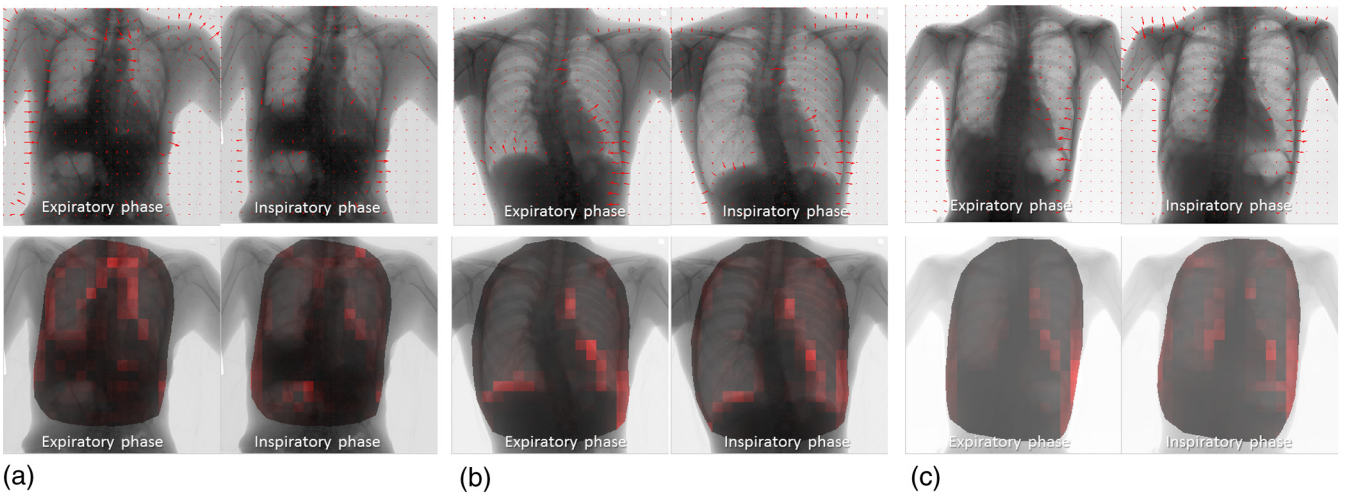

Fig. 9 Velocity vector map (right) and vector magnitude map (left) generated based on velocity vector analysis on conventional dynamic chest images (abnormal subjects). (a) A 75-year-old woman. (b) A 21-year-old man. (c) A 40-year-old woman.

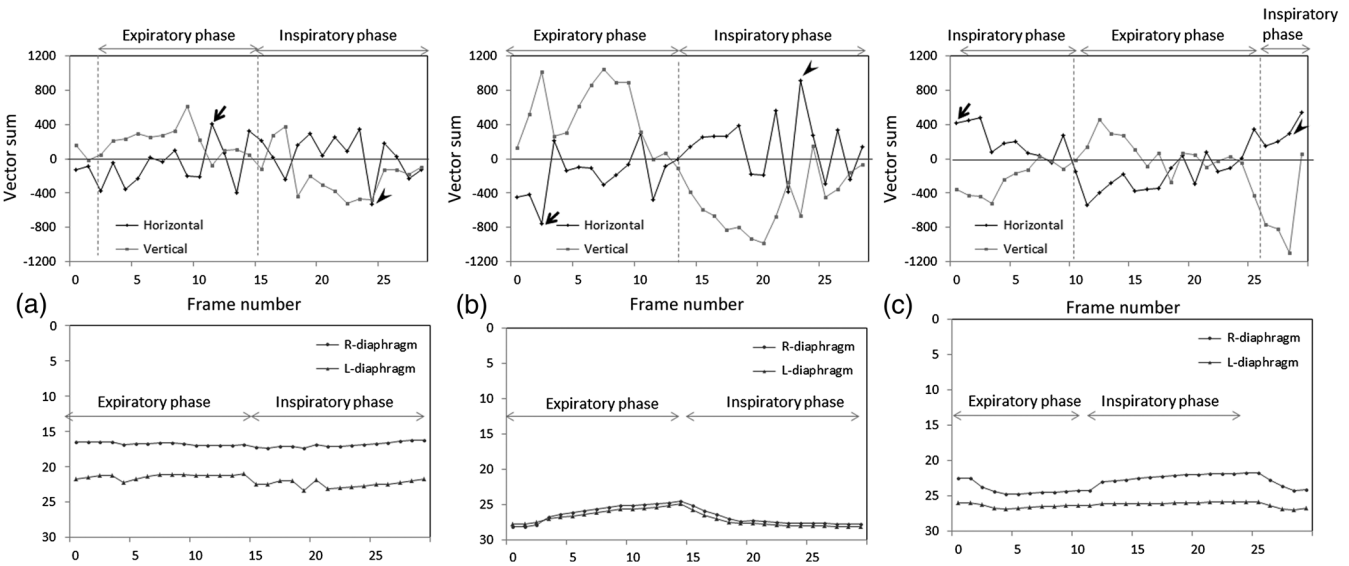

Fig. 10 Vector sum in the horizontal and vertical directions (abnormal subjects). (a) A 75-year-old woman. (b) A 21-year-old man. (c) A 40-year-old woman. The arrows and arrow heads show the frames in expiratory and inspiratory phases indicated in Figs. 6 and 7, respectively.

technical limitations, e.g., the computational time to create a bone suppression image is about 15 s per image and only the frontal view of a chest radiograph can be processed. It is necessary to improve the processing speed and expand the available projection for clinical use. Furthermore, interpretation of dynamic images is both complicated and time-consuming. At present, we could only quantify and visualize rib movement. Thus, to aid radiologists and thoracic physicians to better understand dynamic images, it will also be necessary to develop a computerized method to detect abnormalities, based on nonuniformity, right/left asymmetry, and phase shifting of the velocity field.

5 Conclusions

Dynamic bone images were useful for accurate quantitative analysis of rib movements. With our new analysis technique, rib movements can be quantified and distinguished from those of the other lung structures. Limited rib movements, one of the findings associated with reduced pulmonary function, were indicated as a reduction of rib movement and left/right asymmetric distribution on vector maps. That is, pulmonary impairments could be detected as an exception to a symmetric velocity field of rib movements. Although further studies are required in a large number of patients, the preliminary research indicated the potential clinical usefulness of the rib kinematics obtained from dynamic chest radiography for identifying patients with abnormalities in the lungs.

Acknowledgments

This work was partially supported by the Nakatani Foundation; a Grant-in-Aid for Scientific Research (C) of Ministry of Education, Culture, Sports, Science, and Technology, Japan (Grant No. 24601007); and Canon Inc., Tokyo, Japan. The authors are thankful for the technical support from Yasushi

Kishitani from TOYO Corporation, and staff at the Department of Radiology, Kanazawa University Hospital.

References

1. J. B. West, *Respiratory Physiology—The Essentials*, 3th ed., Lippincott Williams & Wilkins, Philadelphia, Pennsylvania (2000).
2. E. G. Culham, H. A. Jimenez, and C. E. King, "Thoracic kyphosis, rib mobility, and lung volumes in normal women and women with osteoporosis," *Spine* **19**, 1250–1255 (1994).
3. J. C. Leong et al., "Kinematics of the chest cage and spine during breathing in healthy individuals and in patients with adolescent idiopathic scoliosis," *Spine* **24**, 1310–1315 (1999).
4. R. J. Smyth et al., "Pulmonary function in adolescents with mild idiopathic scoliosis," *Thorax* **39**, 901–904 (1984).
5. J. J. Gilmartin and G. J. Gibson, "Abnormalities of chest wall motion in patients with chronic airflow obstruction," *Thorax* **39**, 264–271 (1984).
6. J. J. Gilmartin and G. J. Gibson, "Mechanisms of paradoxical rib cage motion in patients with chronic obstructive pulmonary disease," *Am. Rev. Respir. Dis.* **134**(4), 683–687 (1986).
7. H. Wilkens et al., "Breathing pattern and chest wall volumes during exercise in patients with cystic fibrosis, pulmonary fibrosis and COPD before and after lung transplantation," *Thorax* **65**, 808–814 (2010).
8. R. E. Redlinger, Jr. et al., "Regional chest wall motion dysfunction in patients with pectus excavatum demonstrated via optoelectronic plethysmography," *J. Pediatr. Surg.* **46**, 1172–1176 (2011).
9. A. M. Layton et al., "An assessment of pulmonary function testing and ventilatory kinematics by optoelectronic plethysmography," *Clin. Physiol. Funct. Imaging* **31**, 333–336 (2011).
10. T. Kondo et al., "A dynamic analysis of chest wall motions with MRI in healthy young subjects," *Respirology* **5**, 19–25 (2000).
11. T. A. Wilson et al., "Geometry and respiratory displacement of human ribs," *J. Appl. Physiol.* **62**(5), 1872–1877 (1987).
12. B. Beyer et al., "*In vivo* thorax 3D modelling from costovertebral joint complex kinematics," *Clin. Biomech.* **29**, 434–438 (2014).
13. R. Tanaka et al., "Breathing chest radiography using a dynamic flat-panel detector (FPD) with computer analysis for a screening examination," *Med. Phys.* **31**, 2254–2262 (2004).
14. R. Tanaka et al., "Evaluation of pulmonary function using breathing chest radiography with a dynamic flat-panel detector (FPD): primary results in pulmonary diseases," *Invest. Radiol.* **41**, 735–745 (2006).
15. R. Tanaka et al., "Development of a cardiac evaluation method using a dynamic flat-panel detector (FPD) system: a feasibility study using a cardiac motion phantom," *Radiol. Phys. Technol.* **1**(1), 27–32 (2008).
16. J. Knapp et al., "Feature based neural network regression for feature suppression," U.S. Patent No. 8,204,292 B2 (2012).
17. M. T. Freedman et al., "Lung nodules: improved detection with software that suppresses the rib and clavicle on chest radiographs," *Radiology* **260**, 265–273 (2011).
18. F. Li et al., "Improved detection of subtle lung nodules by use of chest radiographs with bone suppression imaging: receiver operating characteristic analysis with and without localization," *Am. J. Roentgenol.* **196**, 535–541 (2011).
19. R. Tanaka et al., "Improved accuracy of image guided radiation therapy (IMRT) based on bone suppression technique," IEEE 2013 NSS/MIC/RTSD, CFP13NSS-DVD (2014).
20. International Atomic Energy Agency (IAEA), *International Basic Safety Standards for Protection Against Ionizing Radiation and for the Safety of Radiation Sources*," IAEA, Vienna (1996).
21. R. Tanaka et al., "Quantitative analysis of rib movement based on dynamic chest bone images: preliminary results," *Proc. SPIE* **9034**, 903437 (2014).
22. B. Horn and B. Schunck, "Determining optical flow," *Artif. Intell.* **17**, 185–203 (1981).
23. B. Lucus and T. Kanade, "An iterative image registration technique with an application to stereo vision," in *Proc. Seventh Int. Joint Conf. on Artificial Intelligence*, Vol. 2, pp. 674–679 (1981).

Rie Tanaka is an assistant professor of radiological technology at Kanazawa University in Japan. She received her PhD degree in health sciences from Kanazawa University. She has been working on quantitative image analysis of dynamic chest radiography and its clinical evaluation. Her research interests also include observer studies and image-guided radiation therapy. The research presented here was funded by the Cancer Research Foundation.

Shigeru Sanada is a professor of radiological technology at Kanazawa University in Japan. He received his PhD degree in information engineering from the Kanazawa Institute of Engineering, and a doctor of medical science degree from Kanazawa University. He has research interests in developing high-performance screening radiographies, which provide kinetic and three-dimensional information, for lung respiratory and extremity joints movement, and so on, using a dynamic flat-panel detector system. He has published over 150 peer-reviewed papers.

Keita Sakuta is a radiological technologist at Kanazawa University Hospital. He received his PhD degree in health sciences from Kanazawa University. His interests include computer-aided diagnosis and high-resolution computed tomography of the lung and evaluating the image quality of multidetector computed tomography.

Hiroki Kawashima is a radiographer at the Kanazawa University Hospital in Kanazawa, Japan. He holds a PhD degree in health sciences from Kanazawa University. He has research interests in dynamic imaging with flat-panel detectors intended for the chest, wrist, hip, and ankle joint. He collaborates on these mechanisms with orthopedic surgeons, occupational therapists, and engineers.